International Journal of Climatology

International Journal of Climatology RMetS

RESEARCH ARTICLE

Investigating Compound Drought and Hot Extreme Events in Southeast Asia Through Copula Analysis

Lilingjun Liu | Xiaosheng Qin

School of Civil and Environmental Engineering, Nanyang Technological University, Singapore

Correspondence: Xiaosheng Qin (xsqin@ntu.edu.sg)

Received: 19 February 2024 | **Revised:** 14 November 2024 | **Accepted:** 22 January 2025

Funding: This work was supported by Ministry of Education—Singapore.

Keywords: drought | ERA5 | heatwave | hurdle model | SPEI | WBGT

ABSTRACT

The concurrent occurrences of drought and extreme heat events, such as heatwaves, present substantial threats to human health and ecosystems. This study delves into a thorough examination of the collective impacts of drought and extreme heat events in Southeast Asia (SEA) over the past 83 years (1941–2023). Two primary definitions guided the investigation: Compound Drought and Heatwave Events (CDHW) and Compound Hot Droughts (CHD). The Wet-Bulb Globe Temperature (WBGT) was employed to define heatwaves and extreme hot events, while the Standardised Precipitation Evapotranspiration Index (SPEI) was used for drought definition. In addition, the study explored the impact of linear detrending on copula fitting, assessing its effects. The findings of the study consistently revealed a strong positive correlation between drought and heatwaves in CDHW. On the other hand, CHD exhibited varied correlation patterns across regions. Furthermore, the study highlighted that linear detrending had a lower sensitivity in CDHW compared to CHD. The analysis uncovered significant regional disparities in the joint return period ranking of compound events, stemming from diverse copula analysis approaches. Particularly in non-continental SEA, notably in some regions like Sumatra Island, a noteworthy distinction between CDHW and CHD emerged, indicating the limited applicability of CHD in scenarios with stringent concurrence of compound events. These insights provide valuable assistance to the research community, aiding in the discernment of the distinctions between CDHW and CHD in drought and heat-event assessment.

1 | Introduction

Under climate change, the substantial societal and ecological ramifications of climate extremes have garnered significant attention (IPCC 2013). Compound events are typically viewed as the extremes in multiple environmental stressors that are interconnected to epitomise extreme hazardous conditions through four mechanisms that are preconditioned, multivariate, temporally compounding and spatially compounding (Ashfaq, AghaKouchak, and Nguyen 2021; Bevacqua et al. 2021). Compared with single climate extremes, the simultaneous or sequential happenings of these compound extreme events may lead to even greater impacts (Hao, Hao, and Zhang 2020; Hong, Zhang, and Huang 2024). Besides the anticipated escalation of the future risks linked to compound extreme climate events due to global warming's impact and the interplay of physical processes across various scales (Zscheischler et al. 2018), compound extremes have been the most significant climate hazards globally (Hao et al. 2018). As one type of compound event with profound ramifications for both society and the environment, compound drought and heatwaves have drawn strong research attention (Kong et al. 2020; Mukherjee and Mishra 2021; Zhang, She, et al. 2022; Tabari and Willems 2023). The synergetic effects of combined occurrences can overwhelm the resilience thresholds of ecological and socio-economic systems, hence demanding a deeper understanding and strategic management to mitigate the looming risks (Zscheischler and Seneviratne 2017).

Recently, a large number of studies on combined occurrences of droughts and heatwaves and combined instances of dry-hot extremes have been carried out across the world, including China, Brazil, America, Europe and Australia (Sutanto et al. 2020; Alizadeh et al. 2020; Kong et al. 2020; Li et al. 2021; Libonati et al. 2022; Laz, Rahman, and Ouarda 2023). One important aspect of these studies is the investigation of the dependence structure between two single climate extremes through copula analysis (Ribeiro et al. 2020). Due to this advantage, copula analysis has been extensively employed in numerous studies to unravel the complex dynamics of combinative occurrences of drought and heatwave as well as hot and dry extremes. AghaKouchak et al. (2014) introduced a methodology to appraise the risk of compound drought and extreme temperature events using multivariate return periods, thereby establishing a foundational framework for examining combined occurrences of droughts and heatwaves, which has been widely embraced. By emphasising the significance of multivariate approaches in accurately assessing compound climate risks, Zscheischler et al. (2018) further underscored the need for copula-based methods in understanding the interdependencies and heightened frequencies of concurrent hot and dry summers, often overlooked by univariate statistical models. Sarhadi et al. (2018) proposed a non-stationary climate framework, utilising C-vine (canonical vine) copulas to quantify the climate stresses of warm and dry co-occurrences through joint probability. To reveal the effects of combinative drought-heatwave occurrences on social-ecosystem productivity, Yin et al. (2023) utilised an ensemble of 111 simulation members to project the challenges of sustainable development caused by future CDHWs hazards under three SSP scenarios. In this study, the frequency is projected to increase dramatically, by a factor of 10 globally, under the most extreme emission scenario by the end of this century. Zhang et al. (2023) investigated the concurrences of heatwaves and flash droughts in China over the past 60 years. As flash droughts are defined on a weekly basis, this research provided a detailed investigation of compound events on a finer temporal resolution. Besides these highlighted studies, a multitude of research efforts have concentrated on the quantification and characterisation regarding the simultaneous presence of dry and hot extremes in terms of space and time under various climatic conditions, enhancing our understanding of these phenomena in different regions (Zhou and Liu 2018; Chen, Li, et al. 2019; Zscheischler and Fischer 2020; Tavakol, Rahmani, and Harrington 2020).

Previous studies on climate extremes using copula methods generally follow two approaches, namely CDHW and CHD. The CDHW approach focuses on simultaneous drought and heat extremes occurring at a daily scale, demanding a stringent temporal resolution for concurrence (Yin et al. 2022; Ullah et al. 2023). In contrast, CHD studies often examine longer timescales, such as monthly or annually, where a year might be categorised as a CHD year if characterised by overall low precipitation and high temperatures (Zhang, Hao, et al. 2022; Collins 2022). While both focus on the co-occurrence of heat and drought, their different temporal frameworks may lead to instances where the concurrence of extremes in CHD events is overlooked when analysed at a daily level, emphasising a gap in understanding how simultaneous extremes manifest over varying temporal scales. Southeast Asia (SEA), a region heavily impacted by droughts and heatwaves in recent years (D'Arrigo et al. 2006; Miyan 2015; Ullah et al. 2022; Li, Yuan, and Hang 2022), faces even greater challenges due to its dense population (Li et al. 2023). Despite its vulnerability, there remains limited research on the copula-based analysis of these compound events in the region. Therefore, addressing CDHW and CHD through copula methods is essential for improving our understanding of climate vulnerabilities in SEA. In addition, linear detrending has become an important aspect of copula analysis, transforming non-stationary time series into stationary ones by removing trends to enable accurate analysis under the assumption of stationarity. Zscheischler and Seneviratne (2017) used detrending to assess the dependency of climate variables while minimising the confounding effects of climate change, enhancing the interpretation of the underlying correlations. However, detrending has limitations; it may weaken observed correlations in longer-term analyses (Alizadeh et al. 2020) and obscure trends crucial to the studied phenomena (Raffalovich 1994). Despite its widespread use in CDHW and CHD analyses (Zhou and Liu 2018; Chen, Chen, et al. 2019; Tavakol, Rahmani, and Harrington 2020; Zhang et al. 2023), there is a lack of systematic research on its specific impacts within these contexts, highlighting the need for further investigation into how detrending affects correlation analysis in compound extremes research.

Thus, the aim of this study is to conduct a thorough comparative analysis of compound climate extremes, employing copula analysis for both CDHW and CHD events. This research will critically examine and quantify the effects of linear detrending on individual variables within these contexts. The investigation will focus on SEA, using the Standardised Precipitation Evapotranspiration Index (SPEI) to assess drought conditions and the Wet-Bulb Globe Temperature (WBGT) to evaluate heatwave intensities, both derived from ERA5 reanalysis data. The findings will be systematically analysed and interpreted through the lens of the likelihood multiplication factor (LMF) and joint return period. By answering these questions, we hope a new perspective of assessment of combined occurrences of droughts and heatwaves through copula analysis can be established, which will be of great assistance for a more holistic understanding of compound climate extreme events.

2 | Data and Method

2.1 | Study Area

This research covers SEA, spanning from 90° E to 140° E and from 10° S to 30° N. As a region characterised by its predominantly tropical climate, SEA is home to diverse ecosystems. The environmental landscape, including dense rainforests and extensive river systems, contributes to significant climatic variability. Over the years, the region has been increasingly susceptible to severe droughts and heatwaves (Dong et al. 2021; Li, Yuan, and Hang 2022; Phan-Van et al. 2022; Ha et al. 2022). This growing susceptibility is further compounded by rapid urbanisation and a fast-expanding population (Arfanuzzaman and Dahiya 2019; Maja and Ayano 2021), intensifying the urgency to understand and mitigate these climatic extremes.

2.2 | Data

This study employs the ERA5 reanalysis dataset sourced from the European Centre for Medium-Range Weather Forecasts (ECMWF), spanning an extensive period from 1941 to 2023 (Hersbach et al. 2023). This long-term coverage is intentionally selected to ensure a robust fitting of the copula function. The dataset's 0.25°×0.25° spatial resolution encompasses hourly data on 2-m dew point temperature (d2m), 2-m temperature (t2m), wind speed, and solar radiation downwards. They are used for computing WBGT as a measure of heatwaves. In addition, monthly potential evapotranspiration (PET) and precipitation data are utilised to derive the SPEI for evaluation of drought severity. This comprehensive dataset facilitates an in-depth examination of concurrent drought and heatwave occurrences in SEA (Hersbach et al. 2023). In this research, heatwave events are characterised by a percentile approach and are exclusively considered during warm seasons, as the exceedance of WBGT thresholds in cold seasons does not constitute heatwave events. Given the broad latitudinal expanse of SEA, the duration of warm seasons exhibits variation across different regions. To account for this diversity, we delineate the warm season as a 7-month period (Markonis et al. 2021), centred around the month featuring the highest average WBGT value. This ensures that the analysis accurately reflects the regional climatic variations and effectively captures the periods most susceptible to heatwave conditions.

2.3 | Identification of Compound Events

2.3.1 | Drought Index—SPEI

Drought indices are essential tools in hydrology and climatology, providing quantifiable metrics to assess the magnitude, duration and geographical scope of droughts. These indices facilitate a standardised assessment of drought conditions, aiding in effective management and mitigation strategies. Among various indices, the Standardised Precipitation Index (SPI) has gained extensive usage due to its simplicity and effectiveness in measuring rainfall shortfalls across various temporal ranges (McKee, Doesken, and Kleist 1993). To mitigate the limitation of relying exclusively on precipitation-centric indices from SPI, Vicente-Serrano, Beguería, and López-Moreno (2010) introduced SPEI as an enhancement. This metric integrates precipitation and PET, rendering it a more holistic instrument for evaluating droughts, particularly considering the influence of climate change. The inclusion of temperature data through PET allows the SPEI to capture the effects of evapotranspiration on drought severity, which is increasingly relevant under rising global temperatures. This holistic approach provides a more accurate representation of drought conditions, and its utility is reflected in the widespread adoption of SPEI in various drought studies (Beguería et al. 2014; Potopová et al. 2016; Zhao et al. 2017; Li et al. 2020). Therefore, to comprehensively assess the severity of drought under compound events, the SPEI index is selected in this study to address the impacts of precipitation and PET on drought (Vicente-Serrano et al. 2012; Hao and Singh 2015).

Based on precipitation and PET, water balance D can be obtained as follows:

$$D = P - \mathrm{PET} \tag{1}$$

where P is precipitation. The utilisation of water balance instead of original precipitation is aimed to provide a more comprehensive drought assessment than SPI by considering both water inputs (i.e., precipitation) and water demands (i.e., evapotranspiration). The incorporation of PET can make SPEI sensitive to changes in temperature or other climatic variables that may influence drought conditions under climatic changes. Following the calculation of the water balance D, the computation of the SPEI is analogous to the methodology used in the SPI. This involves standardising the water balance values by fitting them to an appropriate probability distribution. Typically, the Fisk distribution, also known as the log-logistic distribution, is utilised for this purpose, with probability density function (PDF) given as (Singh 1998):

$$f = \frac{(\beta/\alpha)\left(D_i/\alpha\right)^{\beta-1}}{\left(1+\left(D_i/\alpha\right)^{\beta}\right)^2} \tag{2}$$

where α and β are scale parameter and shape parameter, which are both positive. After the estimators of these two parameters are computed, the CDF value can be given by (Singh 1998):

$$F = \frac{1}{1+\left(\frac{\hat{\alpha}}{D}\right)^{\hat{\beta}}} \tag{3}$$

Then SPEI can be calculated through the standardisation process using inverse CDF of the standard normal distribution as:

$$\mathrm{SPEI} = \phi^{-1}(F) \tag{4}$$

2.3.2 | WBGT

The WBGT index, incorporating temperature and humidity, offers a comprehensive measure of heat stress. The employment of the WBGT in the study of heatwaves has been extensively validated, offering an enhanced perspective on evaluating heat-related risks as compared to standard temperature-based indices (Heo, Bell, and Lee 2019; Chen, Li, et al. 2019; Heo and Bell 2019; Li, Yuan, and Kopp 2020). WBGT can be calculated by (Yaglou and Minaed 1957):

$$\mathrm{WBGT} = 0.7T_{\mathrm{w}} + 0.2T_{\mathrm{g}} + 0.1T_{\mathrm{a}} \tag{5}$$

where T_{w} and T_{a} are wet- and dry-bulb temperatures (°C), respectively; T_{g} is globe temperature (°C). T_{w} can be calculated by the following equation (Stull 2011):

$$\begin{aligned} T_{\mathrm{w}} = T_{\mathrm{a}} \times \arctan\left[0.151977(\mathrm{RH}+8.313659)^{1/2}\right] \\ +\arctan\left(T_{\mathrm{a}}+\mathrm{RH}\right) - \arctan(\mathrm{RH}-1.676331) \\ +0.00391838(\mathrm{RH})^{3/2}\arctan(0.023101\mathrm{RH}) - 4.686035 \end{aligned} \tag{6}$$

where RH is relative humidity. As relative humidity data is not included in ERA5 reanalysis, it can be calculated via dew point temperature T_d based on the revised Magnus equation (Alduchov and Eskridge 1996):

$$\mathrm{RH} = 100 \times \left[\frac{e^{\frac{17.625 \times T_d}{243.04 + T_d}}}{e^{\frac{17.625 \times T_a}{243.04 + T_a}}} \right] \quad (7)$$

where T_d is the dew point temperature (°C).

T_g reflects the thermal stress from radiation and wind speed, which can be obtained from (Tonouchi, Murayama, and Ono 2006):

$$T_g = T_a + 0.017\mathrm{ssrd} - 0.208\mathrm{va} \quad (8)$$

where ssrd is the solar radiation downwards in W/m^2, va is the wind speed in m/s.

2.3.3 | CDHW and CHD

In this study, CDHW events are conceptualised as simultaneous occurrences of drought and heatwave conditions on a daily basis. Drought is determined using the 1-month SPEI with a threshold value set below zero to indicate drought conditions. Concurrently, a heatwave is recognised during the peak daily WBGT, surpassing the 80th percentile consistently for a period of at least three successive days with a centred 15-day window (Lyon and Barnston 2017). In the study, we set relatively loose thresholds to define drought and heatwaves, compared with conventional cases. This is to enhance the robustness of copula fitting by increasing the number of data points of CDHW events.

To facilitate copula analysis, we proposed a severity index to quantitatively characterise the intensity of drought and heatwave conditions for a given year. It is computed as the cumulative sum of the deviations of the drought or heatwave indices from their respective thresholds aggregated over all days when CDHW events occur. The mathematical express for a specific year can be presented as:

$$S_D = - \sum_{i \text{ in CDHW days}} \mathrm{SPEI}_i - \mathrm{SPEI}_0 \quad (9)$$

$$S_H = \sum_{i \text{ in CDHW days}} \mathrm{WBGT}_i - \mathrm{WBGT}_0 \quad (10)$$

where S_D and S_H are the severity index for drought and heatwave, respectively. To make the physical meaning of severity consistent for both cases, the severity of drought is set to positive so that larger severity values represent more severe conditions. SPEI_0 and WBGT_0 are the thresholds for drought and heatwaves, which are zero and 80th percentile in this study.

The CHD events in this study are identified through the assessment of annual average values of SPEI and WBGT. This approach provides a straightforward way to characterise drought and heatwave conditions on an annual scale. By leveraging the fact that low annual average SPEI values usually signify drought years, while elevated WBGT annual averages indicate heatwave years, our analysis of CHD focuses on the yearly occurrences of these climatic extremes. Therefore, compared with CDHW, which uses severity index to quantify droughts and heatwave events, the annual average of SPEI and WBGT will be used instead in the investigation of the CHD approach. It is important to note that our examination of CHD does not delve into the simultaneous occurrence of drought and heatwave events on a daily basis.

2.4 | Copula Analysis

Introduced by Sklar (1959), the copula serves as a statistical technique within the realm of probability theory that models the dependence between random variables through a multivariate function. Let X and Y denote WBGT and SPEI, respectively; their joint distribution function can be given as:

$$H(x, y) = \mathrm{Prob}(X \le x, Y \le y) = C\left(F_X(x), F_Y(y)\right) \quad (11)$$

where C denotes the copula function that links the marginal distributions of X and Y, represented by $U = F_X(x)$ and $V = F_Y(y)$ where both U and V are uniformly distributed. Combined with Equation (12), the probability of occurrence for a given event in which heatwave and drought conditions exceed corresponding thresholds (i.e., u and v, respectively) can be expressed as (Sklar 1959):

$$p = \mathrm{Prob}(U > u, V > v) = 1 - u - v + C(u, v) \quad (12)$$

Therefore, the return period (RP) for such an event can be obtained as:

$$\mathrm{RP} = \frac{1}{p} \quad (13)$$

To characterise the combined distribution of drought and heatwave events, our initial step involves determining the best-fitting results for their respective marginal distributions. We employ a variety of theoretical univariate distributions, including Normal, Gamma, Weibull, Log-Normal, Generalised Extreme Value (GEV), Beta, and Pearson Type III (Loucks and van Beek 2017). The optimisation of parameters for each distribution model is carried out using the maximum likelihood estimation (MLE) method. The most suitable distribution model is then selected and built upon the Bayesian information criterion (BIC) (Burnham and Anderson 2004). The best marginal distributions of drought and heatwaves characterised by CHD and CDHW over all grid points in SEA can be found in Figures S1 and S2. The copula function C for each grid point in SEA were fitted from nine copula functions listed in Table 1. Afterwards, the best copula for each grid point will be selected based on BIC. Given that the primary goal of this research is to examine the contrast between CDHW and CHD, coupled with the impact of linear detrending, our analysis will cover four modes: CDHW with and without linear detrending, and CHD with and without linear detrending.

The LMF, introduced by Zscheischler and Seneviratne (2017), is employed to quantitatively measure the correlation of compound events (or dependence). LMF is characterised as the ratio of joint probability over theoretical one in the independence case. The

TABLE 1 | Copula functions employed in the study, along with the applicable range of Kendall's tau (Nelsen 2006).

Copula	Kendall's tau range
Gaussian	$(-1, 1)$
Student t	$(-1, 1)$
Clayton	$(0, 1)$
Gumbel	$(0, 1)$
Frank	$(-1, 1)$
Joe	$(0, 1)$
Galambos	$(0, 1)$
Tawn	$(0, 1)$
FGM	$(2/9, 2/9)$
Plackett	$(-1, 1)$

independence case is denoted with independent copula in the following equation (Zscheischler and Seneviratne 2017):

$$C_{\mathrm{Ind}}(u, v) = uv \tag{14}$$

For a given return period RP_0, (i.e., the exceedance probability $p_0 = 1/\mathrm{RP}_0$), if we consider that two individual climate extremes contribute to the compound event equally, we can compute the marginal values u and v, based on the following equation:

$$u = v = 1 - \sqrt{p_0} \tag{15}$$

Substitute the marginals in Equation (13), we can express the exceedance probability for such marginal values under practical copula C as (Zscheischler and Seneviratne 2017):

$$p_1 = 1 - 2\left(1 - \sqrt{p_0}\right) + C\left(1 - \sqrt{p_0}, 1 - \sqrt{p_0}\right) \tag{16}$$

Thus, the LMF is obtained by (Zscheischler and Seneviratne 2017):

$$\mathrm{LMF} = \frac{p_1}{p_0} \tag{17}$$

It should be noted in Table 1 that some copula functions are not applicable to negative correlation (i.e., Kendall's tau $\tau < 0$) between two random variables. The direct fitting of the copula may not obtain the appropriate results due to the inapplicable range. As all of them can be used for positive correlation, to facilitate better copula fitting results, we can construct a positive correlation between variables by setting $v = 1 - \mathrm{CDF}(S_{\mathrm{D}})$, if original marginals u and v are negatively correlated (i.e., Kendall's tau $\tau < 0$). Therefore, the modified LMF expression considering the negative correlation can be given as:

For $\tau > 0$,

$$\begin{aligned} p_1 &= \mathrm{Prob}\left(s_{\mathrm{H}} > S_{\mathrm{H}}, s_{\mathrm{D}} > S_{\mathrm{D}}\right) \\ &= \mathrm{Prob}(u > U, v > V) = 1 - u - v + C(u, v) \end{aligned} \tag{18}$$

$$LMF = p_1/p_0 = \frac{1 - 2\left(1 - \sqrt{p_0}\right) + C\left(1 - \sqrt{p_0}, 1 - \sqrt{p_0}\right)}{p_0} \tag{19}$$

For $\tau < 0$,

$$\begin{aligned} p_1 &= \mathrm{Prob}\left(s_{\mathrm{H}} > S_{\mathrm{H}}, s_{\mathrm{D}} > S_{\mathrm{D}}\right) \\ &= \mathrm{Prob}\left(u' > U, v' > V\right) = v' - C\left(u', v'\right) \end{aligned} \tag{20}$$

$$\mathrm{LMF} = p_1/p_0 = \frac{\sqrt{p_0} - C\left(1 - \sqrt{p_0}, \sqrt{p_0}\right)}{p_0} \tag{21}$$

where $u = \mathrm{CDF}(S_{\mathrm{H}})$, $v = \mathrm{CDF}(S_{\mathrm{D}})$, $u' = \mathrm{CDF}(S_{\mathrm{H}})$ and $v' = 1 - \mathrm{CDF}(S_{\mathrm{SD}})$.

2.5 | Hurdle Model Adoption

In copula fitting for compound events, an underappreciated issue is the absence of compound events in certain years, resulting in some yearly values being zeros. While a few zeros are tolerable, an excessive presence of zeros can significantly undermine the reliability of the marginal fitting process. The excess of zeros obscures the real distribution, leading to a marginal fitting that is both imprecise and fundamentally flawed. As there are few studies that explicitly investigate the adversarial impacts of excessive zeros in yearly value, an approach of marginal distribution fitting utilising a hurdle model will be presented to address this problem. The hurdle model is a statistical technique specially designed to tackle the abundance of zero values in datasets. This approach divides the data into two separate parts: a binary model determines if an observation is zero or a non-zero value; and a truncated count model is applied to assess the size of the observation, provided that it is positive (Ma, Yan, and Weng 2015). In practical study, besides count data, the hurdle model is also extended to semicontinuous data by combining continuous distribution (Hilbe, de Souza, and Ishida 2017).

Let $x = \left(x_1, \ldots, x_n\right)$ be a sample from random variables X_i that are independent and share identical distributions according to the two-part model. The PDF of a hurdle model is given as (Ma, Yan, and Weng 2015):

$$f(x|\,\lambda, \boldsymbol{\theta}) = \begin{cases} 1 - \lambda, & x = 0 \\ \lambda f(x|\,\boldsymbol{\theta}), & x > 0 \end{cases} \tag{22}$$

As the two parts are independent, we can use MLE to estimate parameters λ and $\boldsymbol{\theta}$ as (Eggers 2015):

$$\hat{\lambda} = r \tag{23}$$

$$\hat{\boldsymbol{\theta}} \in \max L(z|\,\boldsymbol{\theta}) \tag{24}$$

where r is the ratio of the number of non-zero yearly values over total years. Thus, the marginal CDF for heatwave, including excessive zeros, can be expressed based on Equation (23) as:

$$\begin{aligned} \mathrm{CDF}\left(S_{\mathrm{H}}\right) &= F(x|\lambda, \boldsymbol{\theta}) \\ &= 1 - \int_x^{+\infty} f(x|\lambda, \boldsymbol{\theta})\mathrm{d}x \\ &= 1 - \lambda \int_x^{+\infty} f(x|\boldsymbol{\theta})\mathrm{d}x \\ &= 1 - \lambda\left(1 - \mathrm{CDF}\left(S_{\mathrm{H+}}\right)\right) \end{aligned} \tag{25}$$

where S_{H+} is the yearly heatwave severity data with all zeros removed. Finally, utilising the hurdle model, the marginal CDF values for heatwave and drought severity with excessive zeros can be given as (for $\tau > 0$):

$$
\begin{aligned}
u &= 1 - r + r\mathrm{CDF}\left(S_{H+}\right) \\
v &= 1 - r + r\mathrm{CDF}\left(S_{D+}\right)
\end{aligned}
\tag{26}
$$

where S_{D+} denotes the opposite value of drought severity data without zero values. Using the previous method introduced, as described by Equations (21), (22) and (26), the marginal CDF value of drought severity can be easily obtained for negative case.

3 | Results

3.1 | Impacts of Return Periods and Detrending on LMF Spatial Patterns

Figure 1 illustrates the analysis of the LMF for compound climate events during warm seasons over SEA. The maps provide insights into the spatial pattern variability and highlight the potential influence of linear detrending on these compound events. As LMF represents the dependency strength between drought and heatwave (or hot extremes), a higher value indicates a stronger likelihood that these two types of events would occur simultaneously rather than independently. By comparing Figure 1a,c, we observe a prevalent positive correlation in CDHW between two climate extremes across the entire SEA, indicated by an all-grid average LMF of 2.033. In contrast, CHD exhibits a mix of positive and negative correlations. The negative correlations, reflected by LMF values below 1, are predominantly observed in eastern Vietnam, Cambodia, Sumantra and Java Islands, and the west of Borneo. The negative correlation seen in CHD reflects the non-concurrent occurrences of drought and hot extremes at an annual scale. In the case of CDHW, there is a higher likelihood of drought and heatwaves happening simultaneously on specific days during warm seasons, leading to a generally positive correlation.

Upon comparing the left panel (not detrended) with the right panel (detrended) of Figure 1, a generally similar spatial pattern of positive or negative correlations is observed. However, concerning CHD, a marginal weakening of positive correlation is found post-linear detrending. This is evidenced by a 0.3% decrease in the averaged LMF value for CHD over negatively correlated grids, reducing from 1.181 (not detrended) to 1.177 (linearly detrended). In contrast, the negatively correlated grids exhibit a significant reduction in correlation levels after linear detrending, with LMF increasing by approximately 7.1% (e.g., from 0.756 to 0.810). In CDHW, characterised by a prevailing positive correlation across the study area, linear detrending has a minimal impact on increasing correlation levels. The average LMF increases by approximately 0.3% (e.g., from 2.033 without detrending to 2.039 with detrending). Comparing this characteristic among different joint return periods, it is manifested that the increase of LMF caused by linear detrending also elevates as the return periods increase (0.5% for 10 years, 0.8% for 20 years). Concerning the different

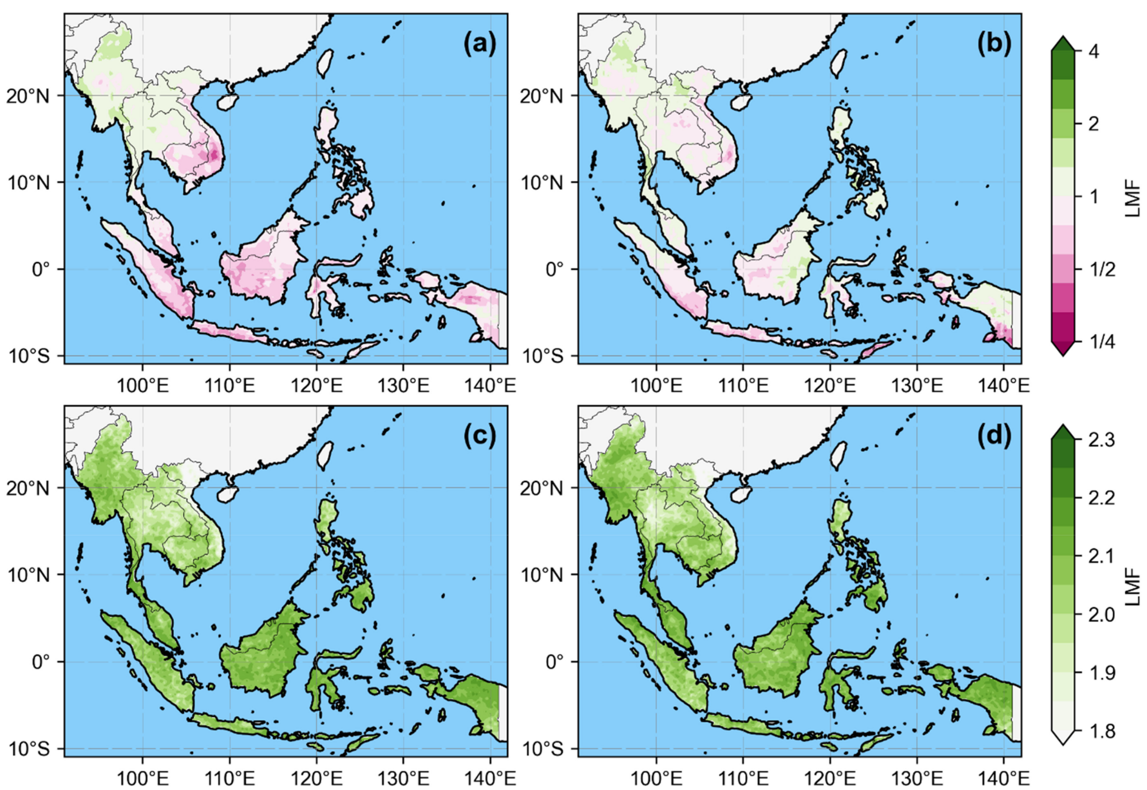

FIGURE 1 | LMF of compound events during warm seasons with RP = 5 years: (a) and (b) are computed with yearly average values based on CHD, and (c) and (d) are calculated from severity values based on CDHW. Please note that in (a) and (c), the WBGT and SPEI are subjected to copula fitting without linear detrending, whereas in (b) and (d), the WBGT and SPEI undergo linear detrending before copula fitting. [Colour figure can be viewed at wileyonlinelibrary.com]

magnitudes of the impact of linear detrending on CHD and CDHW, the lesser influence on CDHW can be attributed to the similar trends in the severity of drought and heatwaves. As both individual climate extremes undergo the removal of similar trends during linear detrending before copula fitting, the combination of marginal distributions remains relatively stable. A comparison of correlation levels under different return periods for compound events yields similar results. Supporting Information provides detailed maps of the spatial pattern of LMF values for other return periods.

3.2 | Joint Dependence Structure Analysis

To delve deeper into the effectiveness of CHD and CDHW in identifying compound events, we have chosen Bangkok as a representative city due to its frequent occurrence of such events. Its geological location is shown in Figure 2. This selection aims to illustrate the evolution of individual events in the city from 1941 to 2023. Figure 3 illustrates the copula analysis outputs in the context of CHD events. The annual average of WBGT and negative SPEI values during warm seasons are illustrated in Figure 3a,b. The higher values of negative SPEI and WBGT represent more severe extreme events. Figure 3c displays the contour lines revealing the joint dependence structure of compound events derived from copula analysis. The differences between the results with and without linear detrending are shown in all subfigures. The influence of linear detrending on WBGT is notably more pronounced compared to its impact on SPEI. This discrepancy is particularly evident during the periods spanning from 1941 to 1970 and from 2000 to 2023. This observation can be attributed to the conspicuous upward trend in temperatures over the past decades in Bangkok, as documented by Marks (2011), with this trend being mitigated by the application of linear detrending. Nevertheless, the long-term fluctuating pattern of drought occurrence does not exhibit the same monotonic clarity observed in temperature trends.

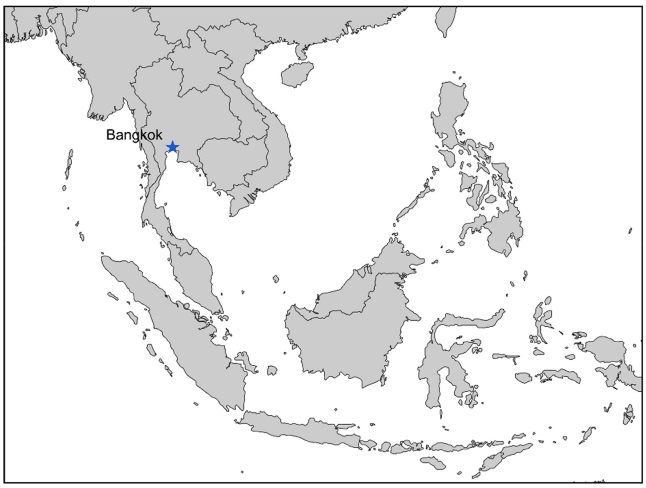

FIGURE 2 | The geological location of Bangkok. [Colour figure can be viewed at wileyonlinelibrary.com]

The joint dependence structure of CHD events, depicted in Figure 3c, illustrates the interconnectedness between the probabilities of both drought and extreme heat events happening. It is found from the contour lines that the extremely hot and drought events are located at the upper right corner. The impact of linear detrending is also evident in the alternation of joint dependence structure. Given that high WBGT values have a reduction, and high SPEI values get amplification after linear detrending, the contour lines of the linear-detrended data move to the left horizontally but exhibit a downward shift vertically. In Figure 3c, the annotations indicate the probability of compound events happening in 2016 for both the non-detrended and linear-detrended cases. To quantify this shift caused by linear detrending in 2016, the univariate return period of WBGT derived from marginal distribution decreases by 74% (from 15.1 to 4.0 years), while the negative SPEI increases by 25% (from 1.2 to 1.5 years). The joint return period of compound events decreases from 56.8 to 10.5 years, with LMF values of 0.32 and 0.58 for non-detrended and linear-detrended conditions, respectively. The LMF values of CHD are lower than 1, representing a negative correlation between drought ant hot extremes in Bangkok.

A similar analysis is conducted for CDHW events, and the outputs are illustrated in Figure 4. The severity indices of drought and heatwaves are used to quantify drought and extreme heat

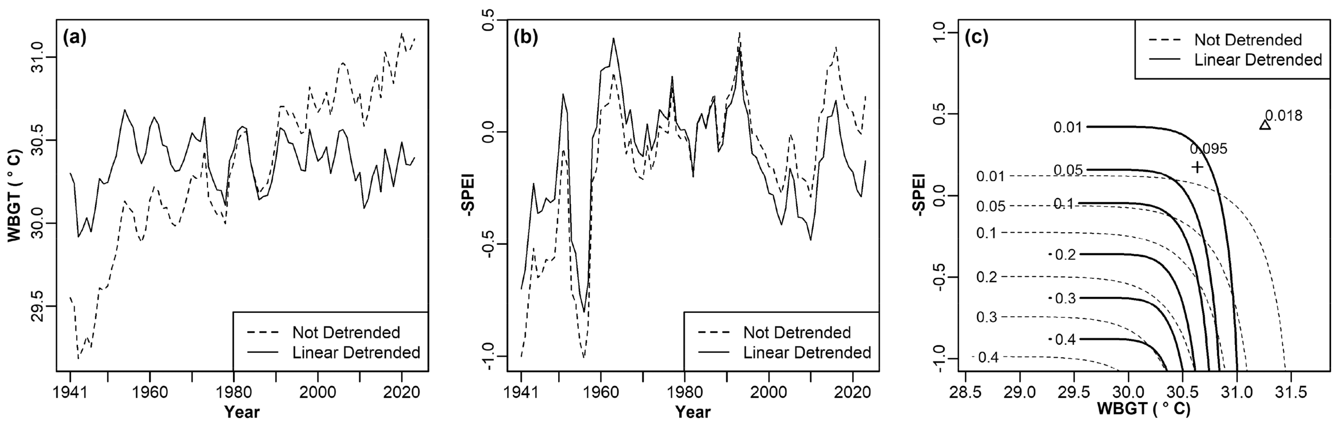

FIGURE 3 | Results of copula analysis for Bangkok grid (100.5018° E, 13.7563° N) in the context of CHD events: (a) WBGT, (b) negative SPEI, (c) the contour line of joint dependence structure. The occurrence probability of compound events in the year 2016 is annotated by a cross (detrended) and a triangle (non-detrended).

events. It is indicated that the two extreme indicators vary wider than the CHD ones. The return periods in the year 2016 for heatwaves and drought are 221.1 and 783.2 years without detrending, and 534.1 and 457.4 years with linear detrending, respectively. Compared with CHD events, the compound events in the year 2016 are measured to be extremely rare under CDHW events, with the joint return period being 24,255 for detrended and 18,085 for non-detrended data. The LMF values for the CDHW event, with and without linear detrending, are 10.07 and 9.58, respectively. The significant amplification of the LMF indicates that in 2016, Bangkok faced a year in which the probability of drought and heatwave events occurring simultaneously on a daily basis was approximately 10 times higher under a joint probabilistic distribution than if they were assumed to occur independently. The positive correlation is shown to be slightly weakened when long-term trends within single events are removed by linear detrending, with LMF decreasing by 5% in Bangkok.

3.3 | Number of Occurrences of Historical Compound Events

To illustrate the evolving spatial patterns of compound events over the past 83 years, Figure 5 maps the occurrences of non-detrended CDHW events under various joint return periods. For brevity, spatial distribution maps for linear-detrended CHD, non-detrended CDH, and non-detrended CDHW events are provided in Supporting Information. Figure 5 illustrates a steady upward trend in compound events across the entire SEA region for all analysed return periods. From 1941 to 2000, most of SEA witnessed no more than three compound events, with some areas even seeing none. However, in the past two decades (2001–2023), there has been a notable surge in compound events. In certain areas, particularly for a 10-year return period, the frequency of CDHWs has surpassed 15 occurrences. Slightly more pronounced increases are observed across northeastern Myanmar, central Thailand, southern Borneo, southern Philippines and southwestern Papua, though the variation across regions remains moderate, leading to a relatively consistent distribution. In addition, higher compound event thresholds (e.g., joint return periods of 20 and 40 years) are associated with lower occurrences of compound events.

Figure 6 shows the number of occurrences of compound events under detrended CDHW, non-detrended CHD and detrended CHD during four consecutive periods under the 10-year return period. When utilising linear-detrended data for copula fitting in CDHW analysis, the upward trend in compound event occurrences becomes somewhat attenuated. For instance, with a 10-year return period, the overall increasing trend persists, albeit with a reduction in the average number of compound event occurrences from 7.5 to 5.3 times over the period 2001–2023. In contrast to the relatively steady level of compound events based on CDHW over the last century, non-detrended CHD exhibits an early spike in the number of occurrences, as shown in Figure 6b,e,h,k. Certain regions, such as eastern Borneo Island and Papua Island, experienced more than 12 compound events during the period 1981 to 2000. Like CDHW, CHD also displays a weakened increasing trend due to linear detrending, but the influence is more pronounced. The average number of occurrences of compound events with return periods of 10 years over SEA in the recent 20 years has been significantly reduced from 12.0 times (non-detrended) to 6.5 times (linear detrended). Notably, in contrast to the lesser impact on LMF observed in the previous analysis for CDHW, CHD appears to be more sensitive to linear detrending. More detailed results under various return periods of both CDHW and CHD can be referred to Supporting Information.

3.4 | The Consistency Between CDHW and CHD

The analysis above highlights distinct characteristics of CDHW compared to CHD events, including variations in LMF values, occurrence probability and the sensitivity to linear detrending. These disparities may be rooted in the inherent definitions of CDHW and CHD. However, it remains unclear whether similar conclusions can be drawn when both assessment tools are employed to evaluate compound event conditions for a specific region. To assess the consistency of these approaches, Bangkok was chosen as a representative city to investigate whether the compound event conditions in different years can be sorted similarly. As depicted in Figure 7, the consistency between CHD and CDHW is visually represented through a quantile–quantile plot. The data points predominantly align with the 45° reference line; notable deviations occur in certain years. Instances of non-concurrent droughts and heatwaves may attenuate the annual severity index and corresponding return periods, resulting in

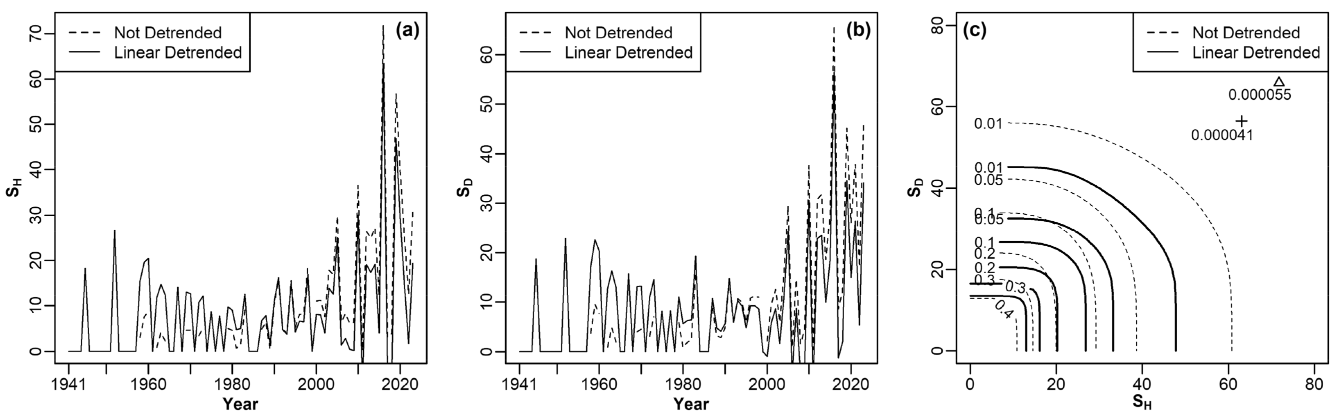

FIGURE 4 | The same as Figure 3, but for CDHW events.

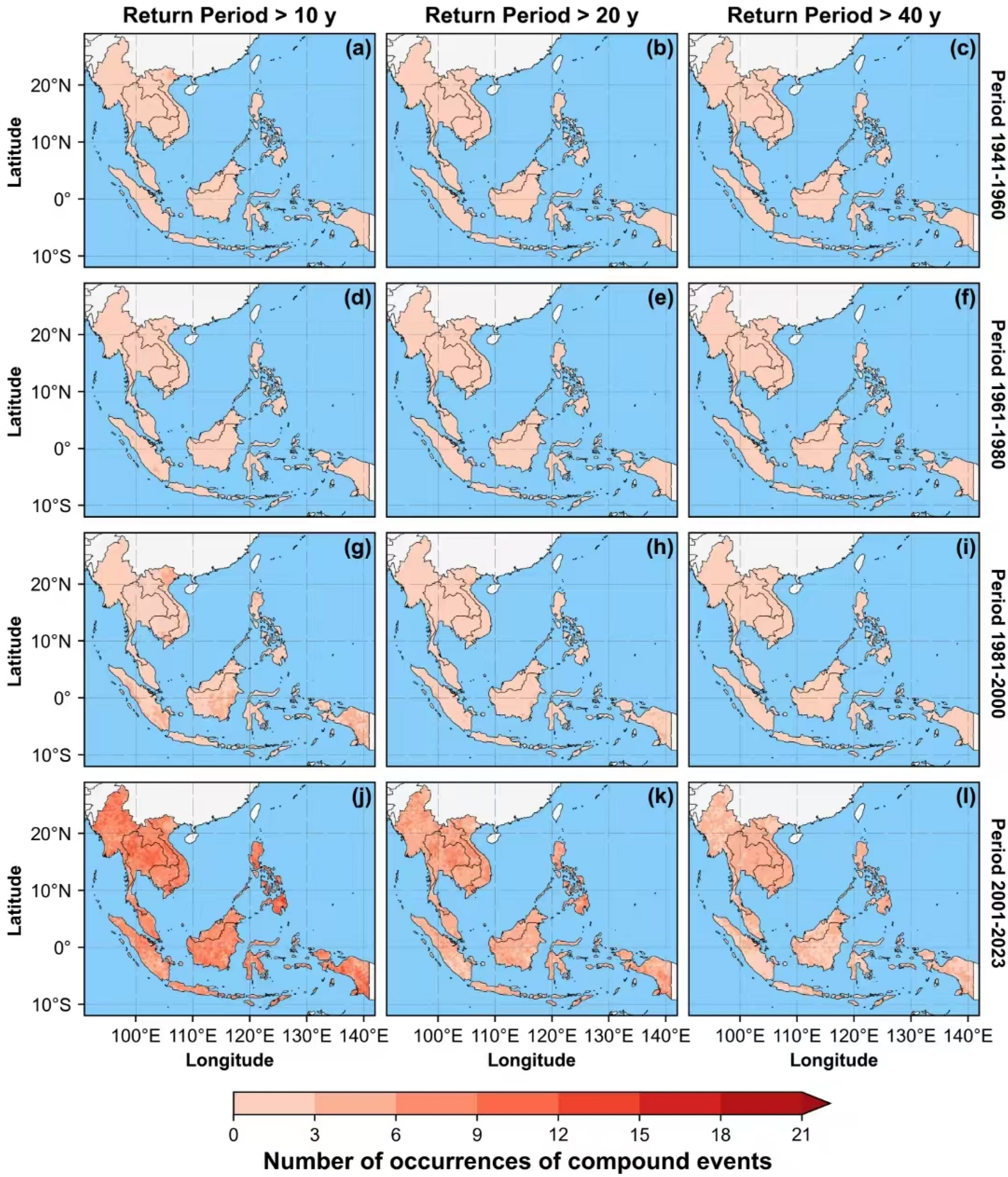

FIGURE 5 | The number of occurrences of compound events based on non-detrended CDHW events: (a), (b) and (c) denote the maps under return periods = 10, 20 and 40 years, respectively, over the period 1941–1960; (d), (e) and (f) show the relevant results over the period 1961–1980; (g), (h) and (i) show the relevant results over period 1981–2000; (j), (k) and (l) show the relevant results over period 2001–2023. [Colour figure can be viewed at wileyonlinelibrary.com]

higher empirical CDF values for CHD compared to CDHW, as observed in the years 1989. Conversely, the simultaneous occurrence of these two extremes within a single year can yield substantial annual severity indices despite the yearly averages of WBGT and SPEI not being markedly high or low. This phenomenon is exemplified by significantly displaced data points below the reference line, as seen in 1945 and 2021. In summary, the two approaches yield approximately analogous assessment results on

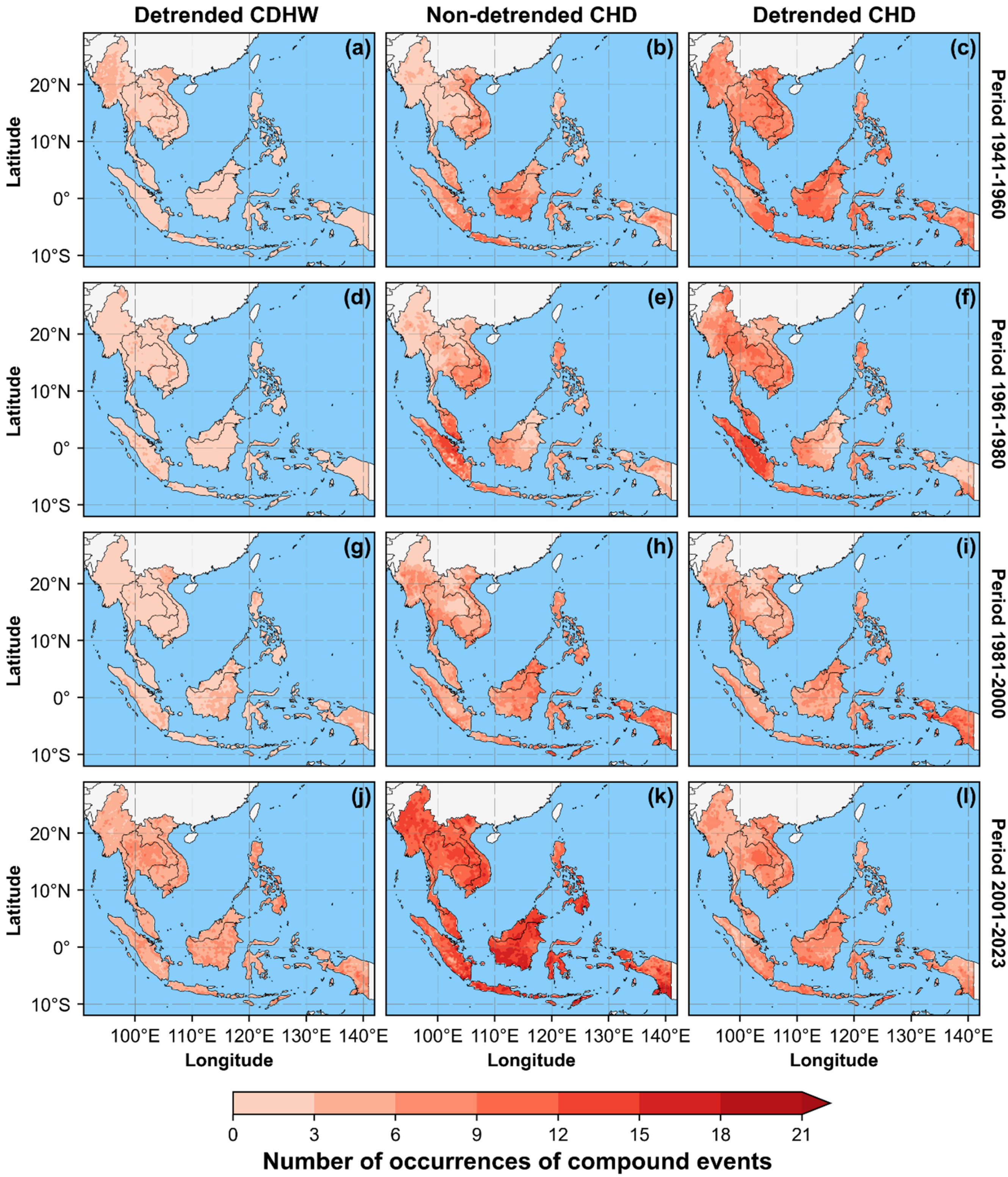

FIGURE 6 | The number of occurrences of compound events under RP = 10 years based on detrended CDHW, non-detrended CHD and detrended CHD. (a), (b) and (c) denote the maps for each mode, respectively, over the period 1941–1960; (d), (e) and (f) show the relevant results over the period 1961–1980; (g), (h) and (i) show the relevant results over period 1981–2000; (j), (k) and (l) show the relevant results over period 2001–2023. [Colour figure can be viewed at wileyonlinelibrary.com]

the compound events conditions among different years, while some substantial deviations between these two approaches also exist for certain years if two extremes do not happen simultaneously on a daily basis.

As the Kendall tau is a widely used non-parametric statistic measuring the ordinal association between two variables (Sen 1968), it serves as the basis for further analysing the consistency between CHD and CDHW. For the selected city, Bangkok, the Kendall tau

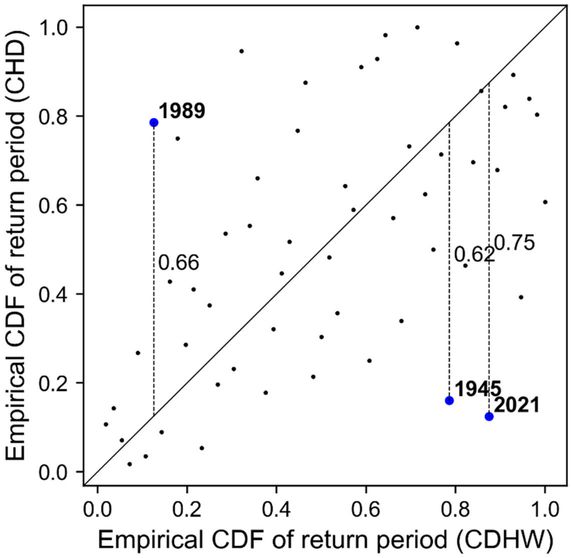

FIGURE 7 | The quantile–quantile plot for CHD and CDHW events in Bangkok over the years show that at least one compound event has occurred. [Colour figure can be viewed at wileyonlinelibrary.com]

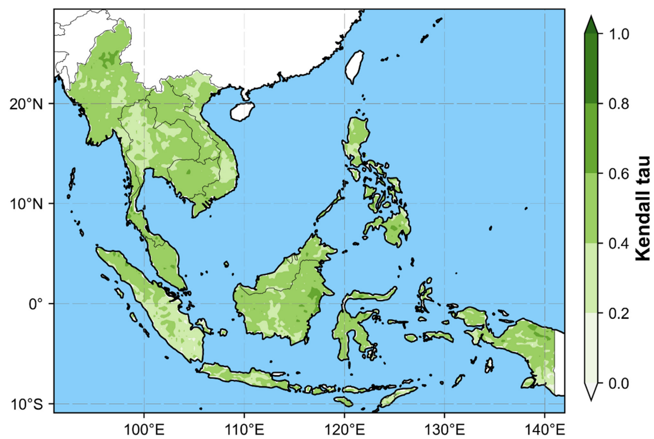

FIGURE 8 | The spatial distribution of Kendall tau between CHD and CDHW over SEA. [Colour figure can be viewed at wileyonlinelibrary.com]

is calculated to be 0.36. Figure 8 illustrates the overall Kendall tau values across the SEA region, showing a general moderate consistency in mainland SEA, the Philippines and Borneo, with Kendall tau values ranging from 0.4 to 0.6. However, regions in the south of Sumatra Island and the northwest of Thailand exhibit more significant inconsistencies between CHD and CDHW, with Kendall tau values below 0.2. The low Kendall tau value in those regions represents a notable discrepancy between CHD and CDHW, which might be caused by the non-concurrent drought and heatwave extremes. Figure 9 shows the latitudinal variation of the number of days in which drought and heatwaves occur concurrently. In this figure, we observe a significant decrease in concurrent days from north to south regions. When two approaches are used to assess the compound events conditions, the low concurrent days will lead to a reduced severity of drought and heatwaves, which is used to measure compound event conditions in the CDHW approach. While, a year will be assessed as severe compound climate extremes under CHD as long as the yearly WBGT and negative SPEI are high. Therefore, the severity

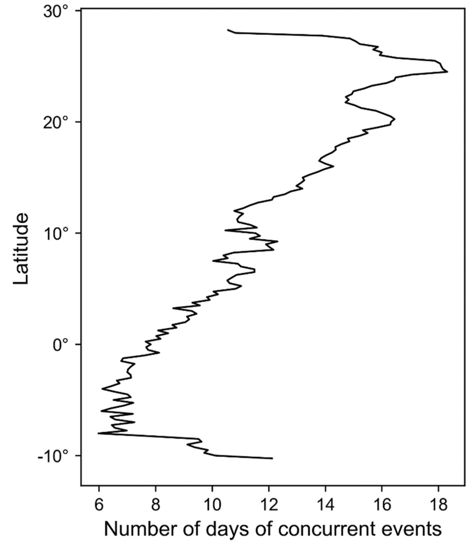

FIGURE 9 | The latitudinal variation of a number of days when drought and heatwave occur simultaneously on the annual average.

of compound events will be underestimated by CDHW due to the lower severity index caused by the reduction of concurrent days, which is shown in Figure 9. Thus, compared with CDHW, CHD may not be an appropriate approach for assessing compound event conditions in this area on a daily basis.

4 | Discussion

In this study, we conducted a comprehensive copula analysis to examine compound dry and hot events in SEA using two distinct definitions: CDHW and CHD. Both definitions apply WBGT to assess heat stress, considering temperature and humidity to provide a more holistic measure of heatwave stress. Concurrently, SPEI is used to assess drought, accurately capturing drought dynamics by integrating precipitation and evapotranspiration data, which offers in-depth insights into moisture deficiencies across different timescales. The combined use of WBGT and SPEI allows for a detailed and contextually relevant characterisation of CDHW and CHD events in the region. By employing joint return periods and LMF, we carefully examine the spatial patterns and temporal trends of these events across SEA. Results from copula analysis are illustrated through LMF values and occurrence frequencies. The observed trends in compound events align with findings from previous correlation-based studies (Mukherjee and Mishra 2021; Zhang, She, et al. 2022; Zhao et al. 2023), showing a generally strong positive correlation between drought and heatwave events over the entire period. Similar findings were reported by Shi et al. (2024), who measured independence using the ratio of drought and heatwave severity indices. Our analysis also reveals a noticeable surge in compound event occurrences, especially for 10-year joint return periods across the region. This trend has been most pronounced in the past two decades, with areas such as Myanmar, Borneo Island, southern Philippines and Papua Island experiencing a substantial rise, with more than 15 CDHW events in the last two decades. The sharp increase in compound events is similarly reflected in CHD, consistent with the findings of Hao et al. (2018).

Another important contribution worth mentioning is the adoption of the hurdle model in this study to improve marginal distribution fitting. A frequently overlooked issue in copula analysis, especially within the CDHW approach, is the substantial impact of excessive zeros on marginal distribution fitting. In the CHD approach, the copula is directly fitted based on the yearly average value of drought or heat extremes, ensuring that each year has a non-zero value. In contrast, CDHW requires the simultaneous occurrence of drought and heatwave, resulting in days being filtered based on their concurrence. Consequently, zero values are inevitable in the CDHW time series, representing years without the simultaneous occurrence of both drought and heatwave on the same day. To address this challenge, zero-inflated models and hurdle models offer effective solutions for fitting distributions in data with a high frequency of zeros. While the zero-inflated model assumes two processes, one generating only zero values and the other generating both zero and non-zero values, the hurdle model assigns all zero values to a single process. Given that the source of zeros in the CDHW approach aligns more closely with the assumptions of the hurdle model, we adopted this model in our study.

In addition, the study highlights key distinctions between CDHW and CHD events. LMF analysis shows negative correlations between drought and hot extremes in CHD for some regions, in contrast to the generally positive correlation observed in CDHW. This negative correlation in CHD differs from the findings of Zscheischler and Seneviratne (2017). While differences in the indices used to characterise drought and hot extremes may explain some of this inconsistency, limitations in the copula functions employed may also play a role. Compound events can occur on specific days when both WBGT and SPEI are high, but CHD, with its coarser annual time resolution, may fail to capture these events, which could explain why CDHW exhibits a stronger positive correlation. In addition, CDHW is less sensitive to linear detrending before copula fitting, as indicated by the LMF analysis. This may be due to the more stable trends in WBGT and SPEI severity over the past decades. In contrast, the stronger temporal variations in individual extremes within CHD result in a more substantial impact on copula fitting and LMF values. Both CDHW and CHD provide similar rankings of compound event conditions across years, though notable discrepancies arise in non-continental areas of SEA, particularly in the southern hemisphere, such as Sumatra and the northwest of Thailand, due to fewer concurrent days of compound events.

In general, our study offers several innovative contributions. First, by defining compound dry and hot events (i.e., CDHW) on a finer time scale (daily basis), we demonstrate its ability to identify compound events with higher resolution, leading to more accurate assessments of compound event conditions, particularly in regions where drought and heatwaves may occur non-simultaneously within a year (e.g., Sumatra Island). Second, the introduction of the hurdle model for marginal distribution fitting in CDHW provides an effective solution to the distortion caused by excessive zeros, offering a valuable alternative for copula analysis with zero-inflated data. Third, we assess the advantages and limitations of linear detrending techniques, showing that while they may reduce the severity of compound events with lower return periods, they strengthen the correlation between the individual events when evaluated using LMF values. Finally, the novel application of both CDHW and CHD in SEA provides unique insights into compound dry and hot event risk assessment, which could be adapted for use in other regions worldwide.

5 | Conclusion

This study presents a thorough comparative analysis of compound dry and hot events in SEA using copula analysis for both CDHW and CHD events. With its finer, daily time scale, the CDHW approach captures compound events at a higher resolution, making it particularly suitable for regions where drought and heatwaves may not occur simultaneously. In contrast, the CHD method, with its yearly time scale, offers a broader perspective on long-term trends, providing valuable insights for regions where seasonal or annual averages are more relevant for assessing risk patterns. The application of a hurdle model for CDHW offers a practical solution for managing zero-inflated data in copula analysis, improving marginal distribution fitting. The necessity of linear detrending is validated in reducing compound event severity at lower return periods while strengthening event correlation when assessed through LMF values.

Our study offers valuable guidance for policymakers and stakeholders. Identifying SEA regions where compound dry and hot events are increasing enables policymakers to focus resources and interventions in high-risk areas. Understanding specific locations and timeframes of heightened compound event helps regional governments and disaster agencies develop targeted action plans, such as promoting drought-resistant agriculture, improving water management, and refining heatwave response protocols to protect vulnerable populations. In addition, our use of joint return periods and LMF analysis offers a quantitative foundation for assessing event likelihood and severity, supporting policy thresholds and infrastructure planning. For example, recognising the increasing frequency of compound events can inform updates to building codes, health advisories, and urban planning standards. Future projections based on these methods could further guide adaptive policies to address anticipated shifts in climate extremes.

While this study provides valuable insights, it also has several limitations that highlight potential avenues for future research. Primarily, it relies on historical data, which constrains its applicability for projecting future climate conditions. To address this, future studies could incorporate predictive climate models, such as CMIP6, to explore how compound dry and hot events might evolve under different scenarios. In addition, the copula methods applied here may not fully capture the nuanced dependencies between drought and heatwave events across diverse spatial and temporal scales; thus, exploring advanced copula techniques or machine-learning approaches could improve accuracy. Finally, the definitions of CDHW and CHD used in this study reflect different timescales and might benefit from validation with finer-scale data to ensure applicability across local contexts in SEA. Addressing these limitations could strengthen the study's methodologies and enhance its practical value for policymakers.

Author Contributions

Lilingjun Liu: conceptualization, methodology, formal analysis, writing – original draft, data curation, investigation. **Xiaosheng Qin:** validation, supervision, funding acquisition, writing – review and editing.

Acknowledgements

This research is supported by Singapore MOE Academic Research Fund Tier 2 (MOE-T2EP50122-0003) and Singapore MOE Academic Research Fund Tier 1 (Grant No. RG72/22). Any opinions, findings and conclusions or recommendations expressed in this material are those of the authors and do not reflect the views of the Ministry of Education, Singapore. The European Centre for Medium-Range Weather Forecasting (ECMWF) is acknowledged for providing ERA5 reanalysis data. We greatly appreciate the reviewers' comments, which have been instrumental in enhancing the quality of the paper.

Conflicts of Interest

The authors declare no conflicts of interest.

Data Availability Statement

The data that support the findings of this study are available from the corresponding author upon reasonable request.

References

AghaKouchak, A., L. Cheng, O. Mazdiyasni, and A. Farahmand. 2014. "Global Warming and Changes in Risk of Concurrent Climate Extremes: Insights From the 2014 California Drought." *Geophysical Research Letters* 41, no. 24: 8847–8852.

Alduchov, O. A., and R. E. Eskridge. 1996. "Improved Magnus Form Approximation of Saturation Vapor Pressure." *Journal of Applied Meteorology and Climatology* 35, no. 4: 601–609.

Alizadeh, M. R., J. Adamowski, M. R. Nikoo, A. AghaKouchak, P. Dennison, and M. Sadegh. 2020. "A Century of Observations Reveals Increasing Likelihood of Continental-Scale Compound Dry-Hot Extremes." *Science Advances* 6, no. 39: eaaz4571.

Arfanuzzaman, M., and B. Dahiya. 2019. "Sustainable Urbanization in Southeast Asia and Beyond: Challenges of Population Growth, Land Use Change, and Environmental Health." *Growth and Change* 50, no. 2: 725–744.

Ashfaq, M., A. AghaKouchak, and P. Nguyen. 2021. *Predictive Understanding of Compound and Cascading Extremes and Their Impacts*. Report No. AI4ESP1006. Oak Ridge, TN/Irvine, CA: Oak Ridge National Lab. (ORNL)/Univ. of California.

Beguería, S., S. M. Vicente-Serrano, F. Reig, and B. Latorre. 2014. "Standardized Precipitation Evapotranspiration Index (SPEI) Revisited: Parameter Fitting, Evapotranspiration Models, Tools, Datasets and Drought Monitoring." *International Journal of Climatology* 34, no. 10: 3001–3023.

Bevacqua, E., C. De Michele, C. Manning, et al. 2021. "Guidelines for Studying Diverse Types of Compound Weather and Climate Events." *Earth's Future* 9, no. 11: e2021EF002340.

Burnham, K. P., and D. R. Anderson. 2004. "Multimodel Inference: Understanding AIC and BIC in Model Selection." *Sociological Methods & Research* 33, no. 2: 261–304.

Chen, L., X. Chen, L. Cheng, P. Zhou, and Z. Liu. 2019. "Compound Hot Droughts Over China: Identification, Risk Patterns and Variations." *Atmospheric Research* 227: 210–219.

Chen, X., N. Li, J. Liu, Z. Zhang, and Y. Liu. 2019. "Global Heat Wave Hazard Considering Humidity Effects During the 21st Century." *International Journal of Environmental Research and Public Health* 16, no. 9: 1513.

Collins, B. 2022. "Frequency of Compound Hot–Dry Weather Extremes Has Significantly Increased in Australia Since 1889." *Journal of Agronomy and Crop Science* 208, no. 6: 941–955.

D'Arrigo, R., R. Wilson, J. Palmer, et al. 2006. "Monsoon Drought Over Java, Indonesia, During the Past Two Centuries." *Geophysical Research Letters* 33, no. 4: L04709. https://doi.org/10.1029/2005GL025465.

Dong, Z., L. Wang, Y. Sun, et al. 2021. "Heatwaves in Southeast Asia and Their Changes in a Warmer World." *Earth's Future* 9, no. 7: e2021EF001992.

Eggers, J. 2015. *On Statistical Methods for Zero-Inflated Models*. U.U.D.M. Project Report 2015:9. Uppsala, Sweden: Uppsala University.

Ha, T. V., J. Huth, F. Bachofer, and C. Kuenzer. 2022. "A Review of Earth Observation-Based Drought Studies in Southeast Asia." *Remote Sensing* 14, no. 15: 3763.

Hao, Z., F. Hao, V. P. Singh, and X. Zhang. 2018. "Changes in the Severity of Compound Drought and Hot Extremes Over Global Land Areas." *Environmental Research Letters* 13, no. 12: 124022.

Hao, Z., F. Hao, and X. Zhang. 2020. "CompoundEvents: An R Package for Statistical Modeling of Compound Climate and Weather Events and Their Impacts." Paper presented at EGU General Assembly Conference Abstracts.

Hao, Z., and V. P. Singh. 2015. "Drought Characterization From a Multivariate Perspective: A Review." *Journal of Hydrology* 527: 668–678.

Heo, S., and M. L. Bell. 2019. "Heat Waves in South Korea: Differences of Heat Wave Characteristics by Thermal Indices." *Journal of Exposure Science & Environmental Epidemiology* 29, no. 6: 790–805.

Heo, S., M. L. Bell, and J. T. Lee. 2019. "Comparison of Health Risks by Heat Wave Definition: Applicability of Wet-Bulb Globe Temperature for Heat Wave Criteria." *Environmental Research* 168: 158–170.

Hersbach, H., B. Bell, P. Berrisford, et al. 2023. "ERA5 Hourly Data on Single Levels From 1940 to Present." Copernicus Climate Change Service (C3S) Climate Data Store (CDS). https://doi.org/10.24381/cds.bd0915c6.

Hilbe, J. M., R. S. de Souza, and E. E. O. Ishida. 2017. *Bayesian Models for Astrophysical Data: Using R, JAGS, Python, and Stan*. Cambridge, UK: Cambridge University Press. https://www.cambridge.org/core/product/identifier/9781316459515/type/book.

Hong, L. M., Z. C. Zhang, and G. W. Huang. 2024. "Characterization of Flood Risk in Japan in Times of Climate Change and Aging Society." *Journal of Environmental Informatics* 44, no. 2: 100–111. http://doi.org/10.3808/jei.202400525.

Intergovernmental Panel on Climate Change. 2013. *Managing the Risks of Extreme Events and Disasters to Advance Climate Change Adaptation. A Special Report of Working Groups I and II of the Intergovernmental Panel on Climate Change*. Cambridge: Cambridge University Press.

Kong, Q., S. B. Guerreiro, S. Blenkinsop, X. F. Li, and H. J. Fowler. 2020. "Increases in Summertime Concurrent Drought and Heatwave in Eastern China." *Weather and Climate Extremes* 28: 100242.

Laz, O. U., A. Rahman, and T. B. Ouarda. 2023. "Compound Heatwave and Drought Hotspots and Their Trends in Southeast Australia." *Natural Hazards* 119: 357–386.

Li, B., K. Liu, M. Wang, Q. Wang, Q. He, and C. Li. 2023. "Future Global Population Exposure to Record-Breaking Climate Extremes." *Earth's Future* 11, no. 11: e2023EF003786.

Li, D., J. Yuan, and R. E. Kopp. 2020. "Escalating Global Exposure to Compound Heat-Humidity Extremes With Warming." *Environmental Research Letters* 15, no. 6: 064003.

Li, J., Z. Wang, X. Wu, J. Zscheischler, S. Guo, and X. Chen. 2021. "A Standardized Index for Assessing Sub-Monthly Compound Dry and Hot Conditions With Application in China." *Hydrology and Earth System Sciences* 25, no. 3: 1587–1601.

Li, L., D. She, H. Zheng, P. Lin, and Z. L. Yang. 2020. "Elucidating Diverse Drought Characteristics From Two Meteorological Drought Indices (SPI and SPEI) in China." *Journal of Hydrometeorology* 21, no. 7: 1513–1530.

Li, X. X., C. Yuan, and J. Hang. 2022. "Heat Wave Trends in Southeast Asia: Comparison of Results From Observation and Reanalysis Data." *Geophysical Research Letters* 49, no. 4: e2021GL097151.

Libonati, R., J. L. Geirinhas, P. S. Silva, et al. 2022. "Assessing the Role of Compound Drought and Heatwave Events on Unprecedented 2020 Wildfires in the Pantanal." *Environmental Research Letters* 17: 015005.

Loucks, D. P., and E. van Beek. 2017. "An Introduction to Probability, Statistics, and Uncertainty." In *Water Resource Systems Planning and Management*, 213–300. Cham: Springer. https://doi.org/10.1007/978-3-319-44234-1_6.

Lyon, B., and A. G. Barnston. 2017. "Diverse Characteristics of U.S. Summer Heat Waves." *Journal of Climate* 30, no. 19: 7827–7845.

Ma, L., X. Yan, and J. Weng. 2015. "Modeling Traffic Crash Rates of Road Segments Through a Lognormal Hurdle Framework With Flexible Scale Parameter." *Journal of Advanced Transportation* 49, no. 8: 928–940.

Maja, M. M., and S. F. Ayano. 2021. "The Impact of Population Growth on Natural Resources and Farmers' Capacity to Adapt to Climate Change in Low-Income Countries." *Earth Systems and Environment* 5: 271–283.

Markonis, Y., R. Kumar, M. Hanel, O. Rakovec, P. Máca, and A. AghaKouchak. 2021. "The Rise of Compound Warm-Season Droughts in Europe." *Science Advances* 7, no. 6: eabb9668.

Marks, D. 2011. "Climate Change and Thailand: Impact and Response." *Contemporary Southeast Asia* 33: 229–258.

McKee, T. B., N. J. Doesken, and J. Kleist. 1993. "The Relationship of Drought Frequency and Duration to Time Scales." In *Proceedings of the 8th Conference on Applied Climatology*, 179–183. Anaheim, CA.

Miyan, M. A. 2015. "Droughts in Asian Least Developed Countries: Vulnerability and Sustainability." *Weather and Climate Extremes* 7: 8–23.

Mukherjee, S., and A. K. Mishra. 2021. "Increase in Compound Drought and Heatwaves in a Warming World." *Geophysical Research Letters* 48, no. 1: e2020GL090617.

Nelsen, R. B. 2006. *An Introduction to Copulas*. New York, NY: Springer.

Phan-Van, T., P. Nguyen-Ngoc-Bich, T. Ngo-Duc, et al. 2022. "Drought Over Southeast Asia and Its Association With Large-Scale Drivers." *Journal of Climate* 35, no. 15: 4959–4978.

Potopová, V., C. Boroneanţ, B. Boincean, and J. Soukup. 2016. "Impact of Agricultural Drought on Main Crop Yields in the Republic of Moldova." *International Journal of Climatology* 36, no. 4: 2063–2082.

Raffalovich, L. E. 1994. "Detrending Time Series: A Cautionary Note." *Sociological Methods & Research* 22, no. 4: 492–519.

Ribeiro, A. F., A. Russo, C. M. Gouveia, and C. A. Pires. 2020. "Drought-Related Hot Summers: A Joint Probability Analysis in the Iberian Peninsula." *Weather and Climate Extremes* 30: 100279.

Sarhadi, A., M. C. Ausín, M. P. Wiper, D. Touma, and N. S. Diffenbaugh. 2018. "Multidimensional Risk in a Nonstationary Climate: Joint Probability of Increasingly Severe Warm and Dry Conditions." *Science Advances* 4, no. 11: eaau3487.

Sen, P. K. 1968. "Estimates of the Regression Coefficient Based on Kendall's Tau." *Journal of the American Statistical Association* 63: 1379–1389.

Shi, P., Y. Li, A. Biswas, K. Wei, and M. Hou. 2024. "Spatial-Temporal Evolution and Intrinsic Drivers of Compound Drought and Heatwave Events in Mainland China." *Science of the Total Environment* 948: 174834.

Singh, V. P. 1998. "Three-Parameter Log-Logistic Distribution." In *Entropy-Based Parameter Estimation in Hydrology*, vol. 30, 297–311. Dordrecht: Springer. https://doi.org/10.1007/978-94-017-1431-0_18.

Sklar, M. 1959. "Fonctions de repartition an dimensions et leurs marges." *Publications de l'Institut de Statistique de l'Université de Paris* 8: 229–231.

Stull, R. 2011. "Wet-Bulb Temperature From Relative Humidity and Air Temperature." *Journal of Applied Meteorology and Climatology* 50, no. 11: 2267–2269.

Sutanto, S. J., C. Vitolo, C. Di Napoli, M. D'Andrea, and H. A. Van Lanen. 2020. "Heatwaves, Droughts, and Fires: Exploring Compound and Cascading Dry Hazards at the Pan-European Scale." *Environment International* 134: 105276.

Tabari, H., and P. Willems. 2023. "Global Risk Assessment of Compound Hot-Dry Events in the Context of Future Climate Change and Socioeconomic Factors." *npj Climate and Atmospheric Science* 6, no. 1: 74.

Tavakol, A., V. Rahmani, and J. Harrington Jr. 2020. "Probability of Compound Climate Extremes in a Changing Climate: A Copula-Based Study of Hot, Dry, and Windy Events in the Central United States." *Environmental Research Letters* 15, no. 10: 104058.

Tonouchi, M., K. Murayama, and M. Ono. 2006. "WBGT Forecast for Preventing Heat Strokes in Japan." Paper presented at Sixth Symposium on the Urban Environment. American Meteorological Society, Section PJ1.

Ullah, I., F. Saleem, V. Iyakaremye, et al. 2022. "Projected Changes in Socioeconomic Exposure to Heatwaves in South Asia Under Changing Climate." *Earth's Future* 10, no. 2: e2021EF002240. https://doi.org/10.1029/2021EF002240.

Ullah, I., X. M. Zeng, S. Mukherjee, et al. 2023. "Future Amplification of Multivariate Risk of Compound Drought and Heatwave Events on South ASIAN Population." *Earth's Future* 11, no. 12: e2023EF003688.

Vicente-Serrano, S. M., S. Beguería, and J. I. López-Moreno. 2010. "A Multiscalar Drought Index Sensitive to Global Warming: The Standardized Precipitation Evapotranspiration Index." *Journal of Climate* 23, no. 7: 1696–1718.

Vicente-Serrano, S. M., S. Beguería, J. Lorenzo-Lacruz, et al. 2012. "Performance of Drought Indices for Ecological, Agricultural, and Hydrological Applications." *Earth Interactions* 16: 1–27.

Yaglou, C. P., and D. Minaed. 1957. "Control of Heat Casualties at Military Training Centers." *Archives of Industrial Hygiene and Occupational Health* 16, no. 4: 302–316.

Yin, J., P. Gentine, L. Slater, et al. 2023. "Future Socio-Ecosystem Productivity Threatened by Compound Drought–Heatwave Events." *Nature Sustainability* 6, no. 3: 259–272.

Yin, J., L. Slater, L. Gu, Z. Liao, S. Guo, and P. Gentine. 2022. "Global Increases in Lethal Compound Heat Stress: Hydrological Drought Hazards Under Climate Change." *Geophysical Research Letters* 49, no. 18: e2022GL100880.

Zhang, Q., D. She, L. Zhang, G. Wang, J. Chen, and Z. Hao. 2022. "High Sensitivity of Compound Drought and Heatwave Events to Global Warming in the Future." *Earth's Future* 10, no. 11: e2022EF002833.

Zhang, X., Y. Liu, Y. Zhu, et al. 2023. "Probabilistic Analysis on the Influences of Heatwaves During the Onset of Flash Droughts Over China." *Hydrology Research* 54: 869–884.

Zhang, Y., Z. Hao, S. Feng, X. Zhang, and F. Hao. 2022. "Changes and Driving Factors of Compound Agricultural Droughts and Hot Events in Eastern China." *Agricultural Water Management* 263: 107485.

Zhao, H., G. Gao, W. An, X. Zou, H. Li, and M. Hou. 2017. "Timescale Differences Between SC-PDSI and SPEI for Drought Monitoring in China." *Physics and Chemistry of the Earth, Parts A/B/C* 102: 48–58.

Zhao, L., X. Li, Z. Zhang, et al. 2023. "Developing a Novel Framework to Re-Examine Half a Century of Compound Drought and Heatwave Events in Mainland China." *Science of the Total Environment* 874: 162366.

Zhou, P., and Z. Liu. 2018. "Likelihood of Concurrent Climate Extremes and Variations Over China." *Environmental Research Letters* 13, no. 9: 094023.

Zscheischler, J., and E. M. Fischer. 2020. "The Record-Breaking Compound Hot and Dry 2018 Growing Season in Germany." *Weather and Climate Extremes* 29: 100270.

Zscheischler, J., and S. I. Seneviratne. 2017. "Dependence of Drivers Affects Risks Associated With Compound Events." *Science Advances* 3, no. 6: e1700263.

Zscheischler, J., S. Westra, B. J. J. M. van den Hurk, et al. 2018. "Future Climate Risk From Compound Events." *Nature Climate Change* 8, no. 6: 469–477.

Supporting Information

Additional supporting information can be found online in the Supporting Information section.